Ultra-violet degradation of polypropylene: 2. Residual strength and failure mode in relation to the degraded surface layer

G. E. Schoolenberg* and H. D. F. Meijer
Department of Industrial Design Engineering, Delft University of Technology, PO Box 5029, 2600 GA Delft, The Netherlands
(Received 21 May 1990; accepted 26 June 1990)

In a previous paper the degradation profile and the thickness of the degraded layer of artificially ultra-violet (u.v.) degraded specimens were described. This paper deals with the effects of the embrittled surface layer on the mechanical properties of degraded polypropylene (PP). The fracture energy of artificially degraded PP specimens was measured and compared to non-degraded specimens with an equivalent notch. Deformation velocity, test temperature, specimen type, thickness and processing conditions were varied. Fracture energies and fracture surfaces of degraded and notched specimens were compared. The results show that, depending on the condition of the embrittled layer and test conditions, the failure properties of the degraded material go through three stages (I, II, III). For short degradation times, there is no effect of degradation (I). For intermediate degradation times, the fracture energy decreases because defects form in the degraded layer (II). The occurrence of the so-called 'crack speed effect' causes an especially drastic reduction of strength. For long degradation times, a regeneration may occur caused by multiple cracking of the degraded layer (III). With respect to mechanical properties it appears better to have a thin severely degraded layer than a thicker, less severely degraded layer.

(Keywords: degradation; polypropylene; mechanical properties)

INTRODUCTION

In general, u.v. degradation of thick polymer parts (>1 mm) is limited to a thin surface layer. However, this layer causes severe embrittlement. Usually the loss in fracture toughness is characterized by a so-called 'half-time' (t_{50}) at which a 50% reduction of the fracture energy is observed. This method gives valuable information on the lifetime of the material and is useful for comparison, but does not state the loadability of a plastic product.

Fracture is usually assumed to occur from surface cracks, which form easily in the degraded layer. As stated hypothetically in previous papers[1,2] the strength will then depend on the crack length, i.e. the depth of embrittlement, and can be calculated by fracture mechanics. Because geometry factors in fracture mechanics are known for many geometries and loading conditions, this opens possibilities to predict the loadability of degraded plastic products.

Therefore it is investigated in this paper whether the strength of degraded material is equal to the strength of non-degraded material in which a crack of the same length as the thickness of the degraded layer is introduced.

Previously[1] the process of formation of the degraded layer was followed and its thickness determined as a function of degradation time. Here, we will try to correlate the residual strength to the condition and thickness of the degraded layer.

EXPERIMENTAL

Materials and specimen preparation

The material was a polypropylene (PP) homopolymer in a stabilized and a non-stabilized grade. It was processed by either injection or compression moulding. The specimens were degraded in a Hanau Xenotest 1200 weathering machine. For further details the reader is referred to previous work[1].

Impact testing (three-point bending and tensile)

The mechanical tests were mainly performed in three-point bending. A hydraulically actuated, instrumented three-point bending test was used, consisting of a hydraulic actuator with a servo-valve for steering and a linear variable displacement transducer (LVDT) for displacement feedback. The hydraulic cylinder is provided with a tup fitted with a piezo element to record the load. The tup, the anvil and the specimen length comply to standards for the Charpy test[3]. The fracture energy is calculated by integrating the load–displacement curve.

Tensile impact tests were performed using a similar set-up. By choosing the right combination of velocity and specimen length, the same strain rates as in the outer fibre in three-point bending were obtained.

Notching

A group of specimens was degraded, another group was notched with a razor blade for comparison. The notches were produced by driving a razor blade into the specimens at high speed. The razor blade was clamped

* Present address: Shell Research BV, PO Box 3003, 1003 AA Amsterdam, The Netherlands

0032-3861/91/030438-07

between two blocks, placed in the middle of the specimens and hit by a falling weight. This made it possible to produce notches of the required small depth with sufficient accuracy and reproducibility, and to ensure the sharpness of the notch. The sharpness was checked by polishing cross-sections of notched specimens.

RESULTS

Fracture energy in three-point bending

The results of specimens fractured in impact ($v = 1.5\ m\ s^{-1}$) and at low deformation rate ($v = 0.01\ m\ s^{-1}$) are compared in *Figures 1* and *2*. Several other velocities (ranging from 0.01 up to 2.5 m s^{-1}) were tested, but these two proved to be representative for 'high' and 'low' velocities within this range. The transition in behaviour occurred at *ca.* 0.5 m s^{-1}.

It is remarkable that in some cases just after the steep decrease of the failure energy from about 200 to 400 h, there is a 'dip' in the curves, and the curve rises again after longer exposure times. This is very pronounced in the injection-moulded non-stabilized specimens at $v = 0.01\ m\ s^{-1}$. The reproducibility of this behaviour was tested by independently moulding and exposing a second series. A possible explanation for this will be given later.

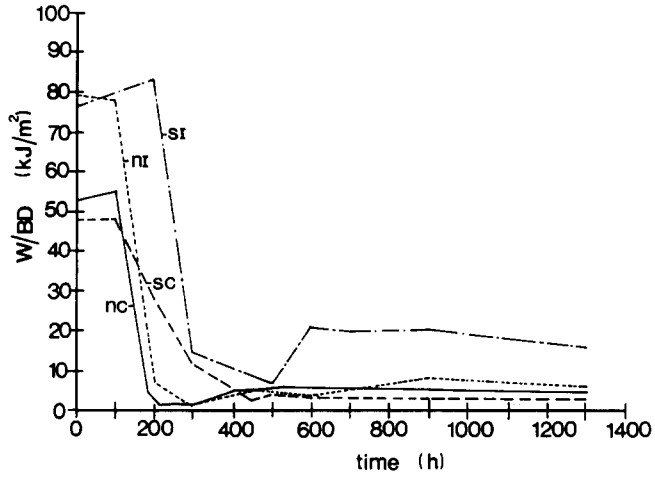

Figure 1 Comparison of the failure energy of the degraded specimens in impact ($v = 1.5\ m\ s^{-1}$) (data points were not drawn for clarity): uc = non-stabilized compression-moulded; sc = stabilized compression-moulded; ni = non-stabilized injection-moulded; si = stabilized injection-moulded

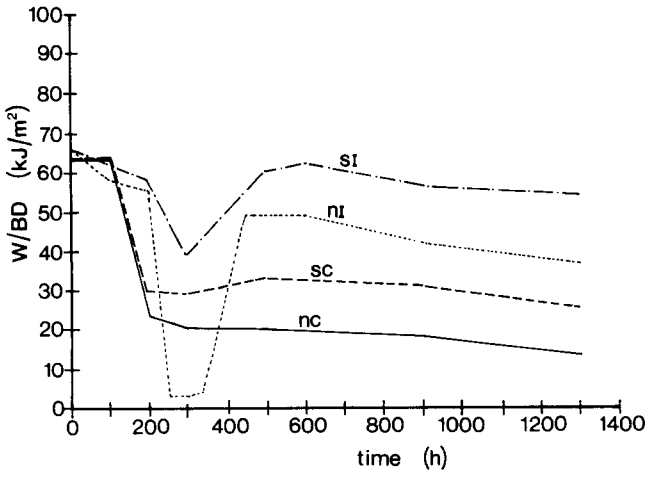

Figure 2 As *Figure 1*, at $v = 0.01\ m\ s^{-1}$

Fracture energy at other test conditions

Tensile tests. Tensile tests showed basically the same results as bending tests. The fracture energy is higher due to the test geometry, but the trends of the curves proved to be the same.

Tests at −45°C. Tests below the glass transition temperature ($T_g \sim -15°C$ for PP), which were performed at −45°C, showed the same behaviour as the tests performed at room temperature and $v > 0.5\ m\ s^{-1}$.

Smaller specimen depths. Specimens of all types with depths of 3 and 2 mm were tested and compared to 4 mm. At $1.5\ m\ s^{-1}$ the behaviour is similar for all the specimens. At $v = 0.01\ m\ s^{-1}$ it is no longer possible to fracture the 2 mm deep specimens, probably because the strain rate and/or the stress level at which the specimens are pushed through the supports of the anvil are too low. It can be concluded that the failure behaviour observed at 4 mm will also occur at smaller depths, if the strain rate is not decreased too much.

Comparison to the notched specimens

Extensive tests on notched specimens were performed. The notches were produced in the same range as the degradation depths found previously[1], i.e. 0.1 to 1 mm.

The fracture energy of notched specimens was directly compared to that of degraded specimens, an example of which is shown in *Figure 3a*. The notch lengths of the notched specimens equal the depth of embrittlement as reported before[1] for the degradation time concerned. In *Figure 3a* the horizontal axes show both the degradation time and the corresponding notch length (equalling the depth of embrittlement). At $1.5\ m\ s^{-1}$ the stabilized and/or injection-moulded specimens showed similar behaviour.

In *Figure 3b* the comparison is made for the fracture energy at the tup velocity of $0.01\ m\ s^{-1}$. It is clear that at this tup velocity the difference between both curves as observed in *Figure 3a* between 200 and 400 h does not occur. On the other hand, there is a much larger discrepancy at longer degradation times, where the notched specimens consistently have a lower fracture energy than the degraded ones. This latter difference also occurs for the other types of specimens and becomes especially large in injection-moulded material, where the behaviour changes from fracture to no fracture (*Figure 3c*). The dip in the curve for the degraded non-stabilized injection-moulded material at 200–300 h causes a large discrepancy between the curves of notched and degraded specimens. Here the fracture energy is only 5% of what is expected compared to the notched specimens.

Classification of the degradation behaviour

It can be concluded that the failure properties of the degraded material go through three stages. Though the relative level of the fracture energies in the different stages may vary with specimen type and deformation rate, they are shown qualitatively in *Figure 4*.

First there is the induction period where the effect of degradation is not yet noticeable (stage I). Then there is the moment of steep decrease of failure properties, usually coinciding with the half-time t_{50}.

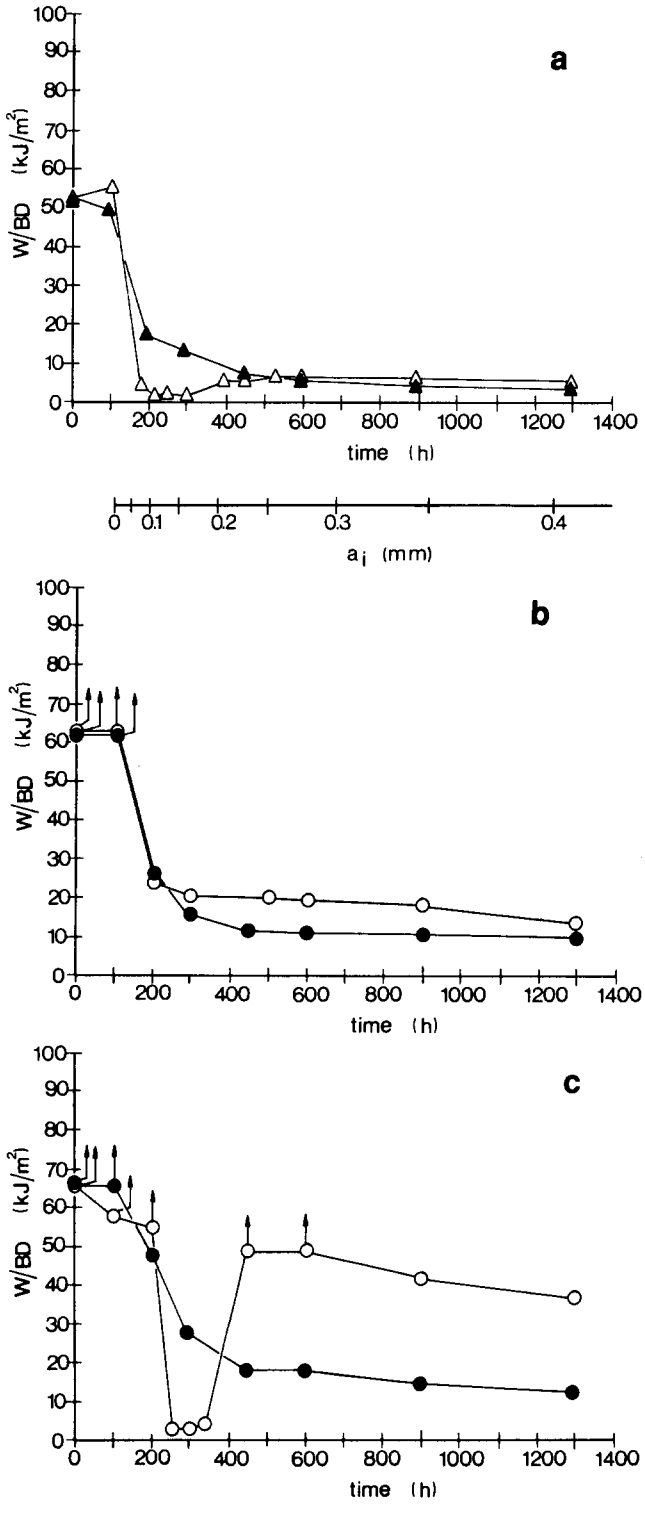

Figure 3 (a) Specific failure energy of notched and degraded specimens compared at 1.5 m s^{-1} and room temperature, for non-stabilized compression-moulded material: (△) degraded specimen; (▲) specimens with equivalent notch (the notch length is equal to the corresponding degradation time). (b) As (a) at 0.01 m s^{-1} and room temperature (vertical arrows indicate that the specimens did not fracture, but were pushed through the supports of the anvil): (○) degraded specimen; (●) specimens with equivalent notch (the notch length is equal to the corresponding degradation time). (c) As (b), for injection-moulded non-stabilized material

After that a stage occurs in which the material shows very brittle behaviour (stage IIb) in the case of non-stabilized material in impact (*Figure 3a*) and for non-stabilized injection-moulded material at lower tup velocities (*Figure 3b*). In this stage the fracture energy is less than that of the specimens with notches equivalent to the depth of embrittlement. In compression-moulded material at $v = 0.01$ m s^{-1} (*Figure 3b*), and in stabilized material in impact, the material is moderately embrittled and the fracture energy about equals that of the notched specimens (stage IIa).

Finally an increase of fracture energy follows, which is particularly pronounced in *Figure 3c*. In this last stage the specific failure energy frequently rises above that of the notched specimens, especially at low tup velocities (stage IIIa), and arrives at a more or less stable end level. At high tup velocities the fracture energy approximates that of notched specimens (stage IIIb).

In *Table 1* the sequence of the stages has been summarized for the different specimens and tup velocities. It is clear that the different stages result from different fracture processes, which will be treated in the following section.

Relation between fracture path, fracture surface and fracture energy

The specimens' fracture surfaces and fracture paths in the stages mentioned above show some interesting differences.

In stage I, specimens fracture in impact only and the fracture surfaces are similar to that of unnotched specimens.

In stage IIb, the fracture energy was much lower than that of the notched specimens and the fracture surface was very smooth (*Figure 5a*). No transition from brittle to ductile material could be observed. The surface is much smoother than that of the notched specimens with equivalent crack length where usually a characteristic

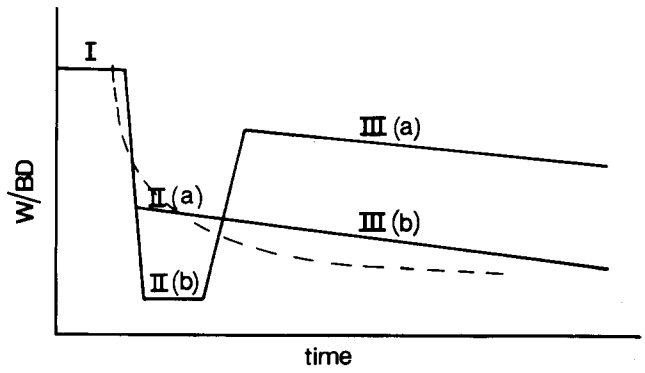

Figure 4 Three stages in the failure behaviour: I, initiation time; IIa, moderately brittle behaviour; IIb, very brittle behaviour; IIIa and IIIb, stable end level. The broken curve is for notched specimens

Table 1 Sequence of the stages of fracture behaviour

Test conditions	Compression-moulded, non-stabilized/ stabilized	Injection-moulded, non-stabilized/ stabilized
Bending		
$v > 0.5$ m s^{-1}, RT	I–IIb–IIIb	I–IIb–IIIb/I–IIa–IIIa
$v < 0.5$ m s^{-1}, RT	I–IIa–IIIa	I–IIb–IIIa
$v > 0.5$ m s^{-1}, −45°C	I–IIb–IIIb	–
$v < 0.5$ m s^{-1}, −45°C	I–IIb–IIIb	–
Tensile		
$v > 0.5$ m s^{-1}, RT	I–IIb–IIIb	–
$v < 0.5$ m s^{-1}, RT	I–IIa–IIIa	–

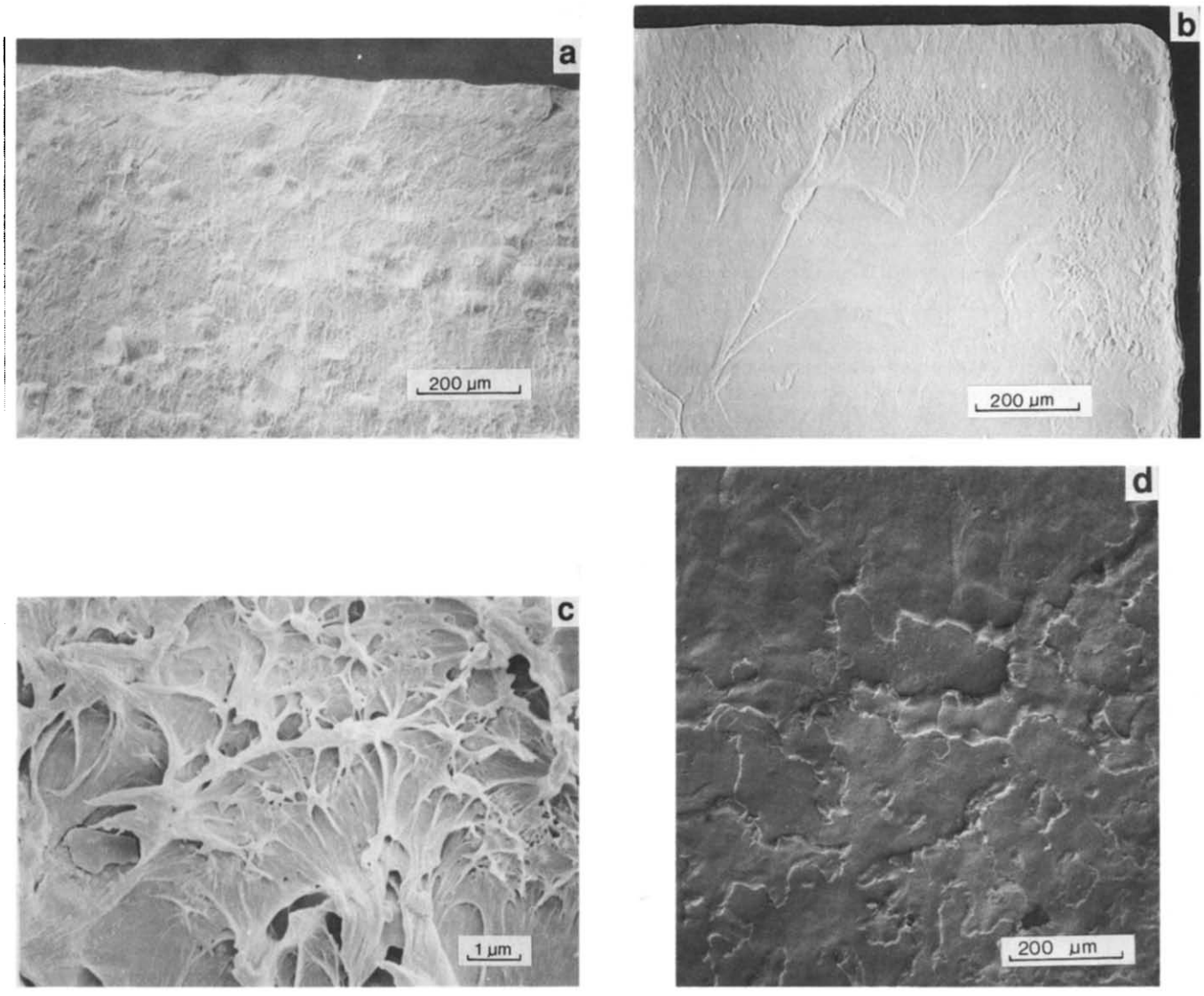

Figure 5 (a) Fracture surface by SEM, for compression-moulded material degraded for 250 h, tested at 1.5 m s^{-1} bending, room temperature. Degraded side on top. (b) As (a), tested at 0.01 m s^{-1}. (c) Detail of fibrillar zone in (b). (d) Detail of patchwork zone below rim (same as (a), tested at 0.01 m s^{-1}, injection-moulded material)

'patchwork zone' is observed[4]. First it was checked whether this might be due to the sharpness of the notch compared to the sharpness of the cracks caused by degradation (see the 'Notching' section above). It was concluded that this cannot be the cause: consequently notched and degraded specimens differ in their fracture behaviour.

Stage IIa occurs in specimens tested at lower velocities and these show a distinct rim as in *Figure 5b* (see also ref. 1, where the non-stabilized compression-moulded material at 250 h was shown as a clear example). This rim appears to be connected to the stage IIa and IIIa behaviour. It is usually followed by fibrillar (*Figure 5c*) and/or patchwork-like (*Figure 5d*) structure, indicating that locally craze formation and/or slow crack growth took place.

At the stage IIIb behaviour (at high deformation rates) no rims or patchwork zones could be observed. The fracture surfaces looked similar to the very smooth ones in stage IIb. In contrast, patchwork zones were observed in the notched specimens at this velocity. The fact that they do not occur in the degraded specimens again indicates a different fracture process. Yet, the fracture energies compare very well.

The rise in fracture energy from the stage IIb to IIIb in bending could be explained by taking a closer look at the fracture paths, illustrated in *Figure 6*. The forked path occurs at high fracture energies, and is also observed in unnotched specimens and specimens with small notches. The S-shaped, asymmetrical paths give lower fracture energies, usually in between that of the notched specimens and the very low fracture energy in the case of straight paths.

Stage IIb results from straight fracture paths, whereas stage IIIb at 1.5 m s^{-1} predominantly shows the higher fracture energy related S-shaped fracture paths.

DISCUSSION

Crack arrest (stage IIa)

The previous section suggests that more than one fracture process is involved. Correspondence between

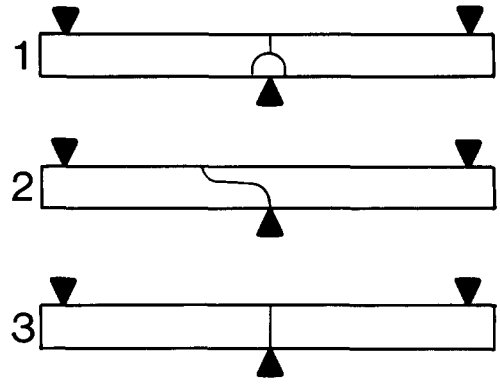

Figure 6 Fracture paths in three-point bending specimens, 1, forked path, rough fracture surface; 2, S-shaped path, smooth fracture surface; 3, straight fracture path, smooth fracture surface

notched and degraded specimens is expected if the embrittled layer fractures spontaneously during degradation, or somewhere in the beginning of the fracture process, and subsequently crack arrest occurs at the interface between brittle and ductile material. If the situation is considered in terms of an energy balance, crack arrest occurs in the case illustrated in *Figure 7a*, where G is the energy release rate, R is the fracture resistance, a_0 is the depth of an inherent flaw (or in degraded material a spontaneous crack) and a_i is the interface from embrittled to ductile material, where a sudden rise in R occurs.

A small surface defect in the embrittled layer is assumed. As soon as $G > R$ at the tip of this initial crack (a_0), crack propagation will begin. G increases with increasing crack length. Thus, more energy than is used up in creating new fracture surface is released. This surplus energy is represented by the left-hand shaded area in *Figure 7a*.

The crack velocity increases, until the interface a_i is reached. From there crack propagation uses up more energy than is supplied. The crack will slow down and eventually arrest. Crack arrest close to a_i is promoted by a small difference between a_0 and a_i and a large difference between the fracture resistances of the degraded and the non-degraded material. In those cases the data of degraded and notched specimens will compare well.

From the correspondence between data for notched and degraded specimens and the fracture surfaces it can be concluded that this type of fracture process occurs in the specimens with forked fracture paths which show type IIa behaviour. Looking at *Table 1* we see that this occurs in a few cases only.

Possibility of dynamic crack propagation effects (stage IIb and IIIb)

The fracture energy of degraded specimens is frequently much lower than of notched specimens. In that case R is obviously very low between a_0 and a_i and the energy gained before the interface is reached should be used up very quickly behind the interface, and the crack should arrest. Apparently this does not occur.

It has previously been suggested by Roland *et al.*[5] that this is caused by a crack speed effect. They argued that the increase of fracture toughness at the interface from embrittled to ductile material will be passed unnoticed, because:

$$K_{Id,brittle} > K_{I,min,ductile} \quad (1)$$

at the interface. Here $K_{Id,brittle}$ is the dynamic stress intensity of the embrittled material at the velocity the crack has achieved once it arrives at the interface, while $K_{I,min,ductile}$ is the minimum K_{Id} value at which the crack in the ductile material achieves a steady state of continuing crack propagation. Because K reduces at high crack velocities, this may occur at a lower K (or R) value than that for crack initiation in the ductile material behind a_i (*Figure 7b*).

For polymers the K *versus* crack speed ($\dot{a}$) relation[6,7] was shown to have a maximum, after which instability occurs and K reduces with $\dot{a}$. If at the moment the crack reaches the interface, $\dot{a} > \dot{a}_{instability}$ and K is larger than the minimum K value for continuing crack propagation, the crack will keep on propagating. Owing to the reduction of K at the instability speed, this may occur at stresses that are smaller than that for crack initiation

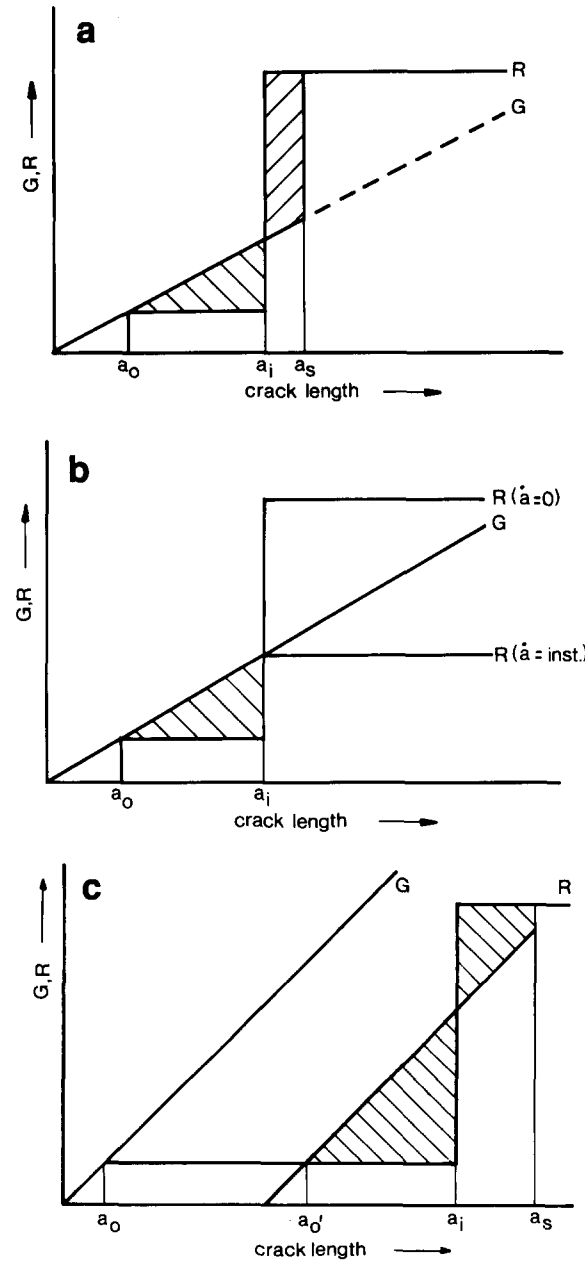

Figure 7 (a) Conditions for crack arrest at the interface between ductile and brittle material. (b) Conditions for the crack speed effect. (c) Conditions for crack arrest due to multiple crack formation

at a_i in the notched material. The argument is analogous when the fracture toughness is expressed in energy terms.

From the test results and the smooth fracture surfaces it can be concluded that this 'crack speed effect' occurs in specimens with straight fracture paths which are in stage IIb.

So and Broutman[8] claim to have observed a similar effect as presented here in ABS and HIPS, coated with SAN and PS respectively. However, in our research a lowering of the failure stress below the yield stress occurs, and this proves that we do not observe a transition from yield to fracture (so the crack arrest case) but that the crack speed effect was actually observed.

From the appearance of the fracture surface the S-shaped paths (occurring in bending in stage IIIb) prove to be due to the crack speed effect as well. These fractures occur because, due to spontaneous crack formation, the probability of the crack speed effect is reduced. There is a competition between fracture by the crack arrest mechanism and the crack speed effect. The load for the occurrence of the crack arrest mechanism is much higher than that for the crack speed effect. If the crack arrests in the centre, further deformation up to the load necessary for fracture by the crack arrest mechanism is necessary. The crack speed effect may occur somewhere else along the specimen length. Thus asymmetric failures arise, giving a smooth fracture surface and a fracture energy between the crack arrest specimens (or notched ones) and the 'crack speed effect' specimens with straight fracture paths.

This mechanism is confirmed by the fact that the centre area in this case shows a multitude of cracks perpendicular to the stress direction, which obviously were arrested[2], whereas no cracks are found in the areas closer to the specimens edges than the S-shaped crack itself.

Another confirmation is derived from the fact that tensile specimens do not show an increase in fracture energy from IIb to IIIb behaviour, and obviously do not show the S-shaped fracture paths.

Multiple crack formation (stage IIIa)

The fracture energy frequently rises above that of notched specimens (stage IIIa). The specimen surface is cracked spontaneously and a multitude of cracks develop during the fracture process. The conditions are favourable for crack arrest. However, the fracture energy may be higher in this stage than that of the notched specimens, because the stress intensity of the main crack, which causes failure, is reduced by that of the adjacent cracks.

The effect of spontaneous cracks can be represented by shifting the origin in the G, R *versus* crack length graphs to the right as done in *Figure 7c*, resulting in crack arrest at the interface. G values for final fracture may be even higher than for the notched specimens, and sometimes specimens even fail to break (e.g. *Figure 3c*).

Fracture energy degradation time relation: summary

The fracture processes described in the previous sections offer an explanation for the rather complex fracture energy–degradation time relations found, compared to the fracture energy of notched specimens. Briefly summarized:

(i) In *stage I* the embrittled layer is not yet thick or brittle enough to cause a reduction of the fracture energy.

(ii) In *stage IIb* the crack speed effect occurs, resulting in very brittle fractures.

(iii) In *stage IIa* and *IIIa* crack arrest occurs causing fracture energies comparable to or higher than that of the notched specimens.

(iv) In *stage IIIb* the crack speed effect remains, and the fracture energy shows a slight increase due to the asymmetric fractures.

Conditions for the crack speed effect

Qualitatively the crack velocity that is achieved at a certain distance from the tip of an initial crack is related to the difference between G and R (*Figure 7a*) and can be derived from simplified dynamic analysis[9]. If the crack propagates from a_0 (the initial crack length) to a_i (the interface), the crack speed at a_i is:

$$\dot{a} = (\pi/k)^{1/2}(E/\rho)^{1/2}(1 - a_0/a_i) \qquad (2)$$

where k is a constant, E is Young's modulus during crack propagation and ρ is the material's density.

In *Figure 8* as an example the relation between the fracture energy (expressed at the strain energy release rate at a_i, as calculated from the fracture energies) and the normalized crack speed is shown for specimens tested at 1.5 m s^{-1} in bending. It shows that a large value of $(1 - a_0/a_i)$ causes very brittle behaviour (low G value). However, a low value of $(1 - a_0/a_i)$ does not guarantee tough behaviour. The data points with both low $(1 - a_0/a_i)$ and low $G(a_i)$ (enclosed by the broken curve) all show the S-shaped paths. This means that spontaneous cracks were present, which are accounted for in the term $(1 - a_0/a_i)$. But the specimens fractured at a site where the crack speed effect occurred, away from the maximum bending moment in the centre, where probably a_0 was smaller (and $(1 - a_0/a_i)$ larger).

Sometimes specimens showing the crack speed effect at high velocities (IIb, IIIb) show crack arrest on lowering the deformation velocity (IIa, IIIa); see *Table 1*. This is remarkable since the ratio a_0/a_i is the same. The explanation may be as follows:

At $v < 0.5$ m s^{-1} the material is above its glass

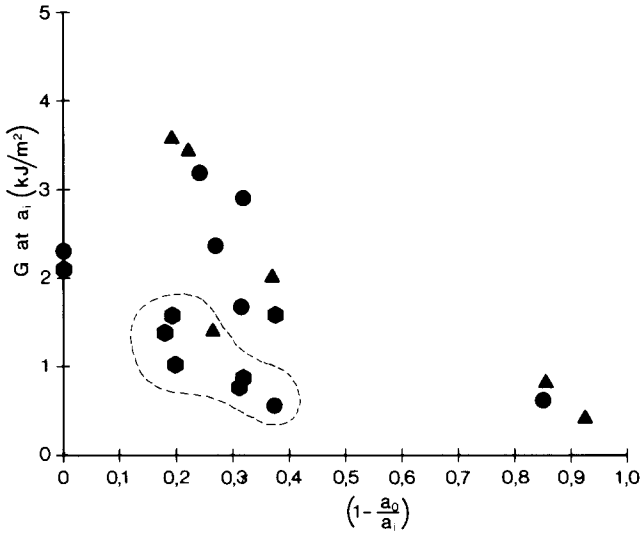

Figure 8 Averages of G at a_i *versus* normalized crack velocity $(1 - a_0/a_i)$ for different specimen types tested at 1.5 m s^{-1}: (●) non-stabilized compression-moulded; (■) stabilized compression-moulded; (▲) non-stabilized injection-moulded

transition temperature, T_g. Crack initiation and instability do not coincide[10] and some stable crack growth occurs, limiting the amount of excess energy stored. Thus the crack velocity at the interface is not high enough, and this leads to crack arrest. Evidence is obtained from the tests at $T = -45°C$, where a transition from crack speed effect to crack arrest on lowering the deformation velocity does not occur (see *Table 1*).

The very low fracture energy dip in *Figure 3c* can be explained from a very high value for the normalized crack speed $(1 - a_0/a_i)$ of 0.8–0.9. The compression-moulded material tested in the same conditions did not show the crack speed effect because the surface layer was more degraded and showed some spontaneous cracks, which reduced the value of $(1 - a_0/a_i)$.

CONCLUSIONS

The degradation behaviour of 2 to 4 mm thick u.v. degraded PP homopolymer specimens can be classified into three stages.

At short degradation times there is no effect of degradation (I). At intermediate degradation times the fracture energy decreases because defects form in the degraded layer (II). This stage can be subdivided according to specimen type and test conditions. In stage IIa the fracture behaviour is similar to that of specimens with an equivalent notch. In stage IIb the occurrence of the so-called 'crack speed effect' causes an especially drastic reduction of strength. At long degradation times an increase in fracture energy may occur caused by multiple cracking of the degraded layer (IIIa). A smaller increase occurs in stage IIIb in bending, due to asymmetric fractures. The correspondence of the fracture energy with notched specimens in stage IIIb is a coincidence.

The transition from stage I to stage II is most important for practical use. Only at low deformation velocities in compression-moulded PP were the fracture behaviour and fracture energy in stage II similar to those of specimens with an equivalent notch. In less notch-sensitive materials this behaviour may be more general, but in PP homopolymer the equivalent notch hypothesis has only limited applicability.

However, the research proved that the crack speed effect is responsible for the very low fracture energy in stage IIb and crack arrest was shown to cause the remarkable regeneration to stage III. To prevent the crack speed effect, theoretically it is beneficial to have a thin and/or severely degraded layer, e.g. by applying strong u.v. absorbers.

REFERENCES

1 Schoolenberg, G. E. and Vink, P. *Polymer* 1991, **32**, 432
2 Schoolenberg, G. E. *J. Mater. Sci.* 1988, **23**, 180
3 DIN 53453
4 Friedrich, K. Thesis, Univ. Bochum, 1978
5 Roland, L., Thomson, K., Mostovoy, S. and Broutman, L. Conf. Proc. Deformation, Yield and Fracture of Polymers, PRI, Cambridge, 1982
6 Marshall, G. P., Couts, L. H. and Williams, J. G. *J. Mater. Sci.* 1974, **9**, 1409
7 Williams, J. G. Int. Conf. on Fracture, New Delhi, 1984, pp. 731–49
8 So, P. and Broutman, L. J. *Polym. Eng. Sci.* 1972, **16**, 2623
9 Mott, N. F. *Engineering (Lond.)* 1948, **165**, 16
10 Schoolenberg, G. E. Thesis, Univ. Delft, 1988